An analytical expression for the J2-integral of an interfacial crack in orthotropic bimaterials

DOI:
10.1111/ffe.12587

Document Version
Accepted author manuscript

Citation for published version (APA):
Tafreshi, A. (2017). An analytical expression for the J2-integral of an interfacial crack in orthotropic bimaterials. *Fatigue & Fracture of Engineering Materials and Structures* , *40*(9), 1443–1458. Advance online publication. https://doi.org/10.1111/ffe.12587

Published in:
Fatigue & Fracture of Engineering Materials and Structures

An analytical expression for the J_2-integral of an interfacial crack in orthotropic bimaterials

A Tafreshi

orcid.org/0000-0001-6065-7459

School of Mechanical, Aerospace and Civil Engineering

University of Manchester, M13 9PL

atafreshi@manchester.ac.uk

This paper presents a new analytical expression relating the J_2-integral and stress intensity factors(SIF) in an in-plane traction free crack between two orthotropic elastic solids using the complex function method. The singular oscillatory near tip field of a bimaterial interfacial crack is usually characterized by a pair of SIFs. In linear elastic interfacial fracture mechanics, the majority of numerical and experimental methods rely on the analytical equations relating J_k-integrals and SIFs. Although an analytical equation relating J_1-integral or strain energy release rate and SIFs is available, a similar relation for J_2-integral in debonded anisotropic solids is non-existent. Using this new analytical expression, in conjunction with the values of J_k, the SIFs can be computed without the need for an auxiliary relation. An example with known analytical solutions for SIFs is presented to show the variation of the J_2-integral near the crack tip of a bimaterial orthotropic plate. Different bimaterial combinations are considered and the effect of material mismatch on J_k is demonstrated.

Keywords

Bimaterial interface crack, debonded dissimilar anisotropic materials, J_k-integral, mixed mode fracture, orthotropic materials, stress intensity factor

NOMENCLATURE

a	=	half crack length or crack half chord length
a_k	=	local coordinates at the crack tip
A_{jk}	=	complex constants
B_{jk}	=	complex constants
$D_j(z)$	=	comlex functions
$d_{jk}(z)$	=	complex functions
E_j	=	modulus of elasticity in the x_j direction
$f_j(z)$	=	complex functions
g(z)	=	complex vector $g(z) = B\begin{bmatrix} f_1\ (z) \\ f_2\ (z) \end{bmatrix}$
G(z)	=	complex vector $G(z) = g'(z) = B\begin{bmatrix} f_1'\ (z) \\ f_2'\ (z) \end{bmatrix}$
G_{12}	=	Shear modulus
H_{jk}	=	real constants
i	=	$\sqrt{-1}$
J_k	=	(k=1,2), J_k-Integrals
K_1, K_2	=	modes 1 and 2 stress intensity factors, respectively
M_{jk}	=	complex functions
(n)	=	material number
n_k	=	direction cosines of the unit outward normal vector to the surface of the elastic body
p_j	=	$\mathrm{Im}(\mu_j)$
P_{jk}	=	complex constants
q_{jk}	=	real constants
Q_{jk}	=	real constants
r	=	small radial distance from the crack tip
s_{jk}	=	elastic compliance matrix (j,k=1,2,6)
		$S_{11} = \frac{1}{E_1} \qquad S_{22} = \frac{1}{E_2} \qquad S_{66} = \frac{1}{G_{12}} \qquad S_{12} = -\frac{\nu_{12}}{E_1} = -\frac{\nu_{21}}{E_2}$
t_j	=	traction vector
u_j	=	displacement vector

x_j = rectangular Cartesian coordiantes

W = strain energy density

$\Upsilon(z)$ = Complex matrix function

z_j = complex coordiantes $(z = x_1 + ix_2)$

α_{jk} and β_{jk} =real constant matrices

β_0 = bimaterial constant

Δ_{jk} = Hermitian matrix ($\Delta = H + iQ$)

ε = bimaterial constant

ε_{jk} = strain tensor

$\phi(z)$ = complex function

$\psi(z)$ = complex function

μ_s = roots of the characteristic equation

ν_{jk} = Poisson's ratio

Ω = +1 and -1 for materials 1 and 2, respectively.

θ = Polar coordiante

σ_{jk} = stress tensor

σ_{x0}, σ_{y0} = Normal stress components in the x- and y-directions

$\omega_{\varepsilon_{jk}}$ = Matrix of real constants

INTRODUCTION

Laminated composite materials are widely used in engineering industries such as aerospace, marine and automobile. This is due to their high specific strength and stiffness. Layered dissimilar anisotropic materials also have a variety of applications in electronic devices such as micro-electro-mechanical systems (MEMS), semiconductors and optical electronics. However, debonding or cracking is the most common type of failure in layered materials during manufacturing or in-service applications. Williams[1] was the first scientist to discover that the stress field along an interface crack between two dissimilar elastic materials is not only singular, but also has an oscillatory behavior of type $r^{-\frac{1}{2}+i\varepsilon}$ where r is the radial distance from the crack tip and ε is a bimaterial constant. His analytical approach was followed by Rice and Sih[2], Erdogan and England[3-5] who mainly focused on linear elastic interfacial fracture mechanics

(LEIFM) of isotropic materials. Clements [6] and Willis[7] extended the problem studied by England for dissimilar anisotropic materials. Wu[8], Qu and Li[9], Qu and Bassani[10], Suo[11], Ting[12-13] , and Beom and Atluri[14] expanded the theories of LEIFM for debonded anisotropic bimaterials. Following their pioneering research a variety of analytical and numerical approaches have been employed in this field[15].

A bimaterial interface crack induces both opening and shearing behaviours even for a single mode loading. The strain energy release rate (SERR) per unit of the crack extension and stress intensity factors (SIFs) are of fundamental importance in the prediction of brittle failure using LEIFM. These depend on the crack geometry, associated loading and material properties. K_1 and K_2 are the mode I and mode II SIFs, respectively. They characterize stress fields in the vicinity of the crack tip with respect to a local Cartesian system (a_1, a_2) that has its origin at the tip of the crack. a_1, a_2 are the axes in the tangent and transverse directions of the crack, respectively.

At present, the most commonly used method in industry for fracture analysis is the J_1-integral which is only applicable to straight cracks. Although it is less sensitive than the displacement method to the mesh size of the crack tip, it would still require stress analysis at internal points and fine contours around the crack front. Additionally, for mixed mode problems, auxiliary equations are required to decouple SIFs. An alternative is to evaluate the J_2-integral for separating SIFs. The J_2-integral not only involves the computation of stresses and strains at a series of internal points around the crack but also the evaluation of highly singular integrals over the crack surfaces. For elastic problems with a straight crack, SERR is the same as J_1-integral which is the Rice's path independent integral[16-17]. This method was first developed by Rice to characterize fractures for two-dimensional (2D) isotropic and homogeneous structures with linear and non-linear elastic material behavior.

A study by the author[18] presents the novel application of the boundary element crack shape sensitivities (BECSS) for the evaluation of the J_1-integral in homogeneous and anisotropic materials where the crack of an arbitrary shape, straight or curve, was treated as the shape design variable. In another study[19] , using the BECSS coupled with an optimization algorithm and an automatic mesh generator, the crack kink angle and crack propagation path in anisotropic and homogeneous elastic solids were predicted. The maximum SERR criterion, best suited for anisotropic structures, was employed. In contrast to the J_1-integral method, the computation of stresses and strains at a series of internal points during the automatic incremental procedure was not required. By direct differentiation of the structural response[20-23] the SERR at the existing crack tip and new cracks for the period of crack growth were determined. However, for decoupling of SIFs[18-19], it was necessary to develop an auxiliary relationship in terms of displacement ratios near the crack tip to be used with the computed J_1 to separate SIFs. In Ref.[24] this deficiency was overcome by direct evaluation of the J_2-integral using BECSS for isotropic and homogeneous materials. It was mathematically proved that the derivative of the total potential energy with respect to the transverse direction of the crack is not the J_2-integral. However, by addition of an integral, involving the strain energy discontinuity, to this derivative, the J_2-integral can be efficiently evaluated. This algorithm was then expanded and applied to the fracture analysis of interfacial cracks of dissimilar isotropic materials[25]. For bimaterials, it was proved that J_2 is equal to the summation of the derivative of the total potential energy with respect to the transverse direction of the crack and two integrals involving crack tip elements. These integrals were related to the jump of displacement derivatives or strains across the interface and also the strain energy density (SED) discontinuity on the crack surfaces and interface region. The results show that the method is simple, accurate, flexible and applicable to both straight and curved cracks. Due to its generic nature, this algorithm[25] can be expanded and applied to the fracture analysis of debonded anisotropic materials. However, an analytical expression relating J_2 and SIFs is required to separate and calculate the corresponding SIFs which at present is non-existent.

In LEIFM, the majority of numerical and experimental methods rely mainly on the employed asymptotic field characterizing the stress and strain in the vicinity of the crack tip, and/or the analytical equations relating J_k-integrals and SIFs. For a linear elastic, isotropic and homogeneous material in mixed mode fracture, the SIFs and J_k-integrals are directly related and the corresponding analytical expressions are available[26]. Malyshev and Salganik[27] derived an analytical expression relating J_1 and SIFs for an interfacial crack between two dissimilar homogeneous and isotropic materials. Gosz et al[28] and Khandelwal and Chadra Kishen[29] obtained an analytical expression for J_2-integral in terms of SIFs for an interfacial crack between two dissimilar homogeneous and isotropic materials using the complex variable method. Wang et al[30] and Chu and Hong[31] showed that the J_k-integrals of a crack in a homogeneous anisotropic structure can be directly related to the corresponding SIFs. Wu[8] and Suo[11] presented an analytical expression for J_1 for an interfacial crack between two anisotropic bimaterial solids. For an interfacial crack in anisotropic bimaterials, the displacement and traction data near the crack tip are usually employed to compute SIFs[32-37] .

This paper presents a new analytical expression relating the J_2-integral and the SIFs in an in-plane traction free crack between two orthotropic elastic solids using the complex function method. Using this new analytical expression, in conjunction with the values of J_k, allows for the computation of the corresponding SIFs without the need for an auxiliary relation.

PLANE BIMATERIAL ANISOTROPIC ELASTICITY

By combining the stress-strain relations, the compatibility equation of strains, and the equilibrium equation, the governing equation for the two-dimensional (2D) plane stress or plane strain state of homogeneous and anisotropic elasticity can be obtained[38]. To have a solution for the stress function, the following characteristic equation must be zero.

$$S_{11}\mu^4 - 2S_{16}\mu^3 + \left(2S_{12} + S_{66}\right)\mu^2 - 2S_{26}\mu + S_{22} = 0. \qquad (1)$$

S_{jk} are the elastic compliances of the material. Lehknitskii[38] has shown that for an anisotropic material, these roots are distinct and must be purely imaginary or complex. However, for a specially orthotropic material, these roots are purely imaginary

$$\mu_1 = ip_1 \quad , \quad \mu_2 = ip_2 \quad , \quad \mu_3 = \bar{\mu}_1 \quad , \quad \mu_4 = \bar{\mu}_2 \qquad (2)$$

where p_1 and p_2 are real numbers.

For 2D in-plane linear elastic, homogeneous and anisotropic materials, the stress (σ_{jk}) and displacement fields (u_j) can be formulated[11, 39-40] in terms of two complex analytical functions $f_j(z_j)$ of the complex variable $z_j = x_1 + \mu_j x_2 \; (j = 1,2)$ as

$$u_j = \begin{bmatrix} u_1 \\ u_2 \end{bmatrix} = 2\,\mathrm{Re}\left\{ A \begin{bmatrix} f_1(z_1) \\ f_2(z_2) \end{bmatrix} \right\} \tag{3}$$

$$[\sigma_{j2}] = \begin{bmatrix} \sigma_{12} \\ \sigma_{22} \end{bmatrix} = 2\,\mathrm{Re}\left[B \begin{bmatrix} f_1'(z_1) \\ f_2'(z_2) \end{bmatrix} \right] \tag{4}$$

$$[\sigma_{j1}] = \begin{bmatrix} \sigma_{11} \\ \sigma_{21} \end{bmatrix} = -2\,\mathrm{Re}\left[BP \begin{bmatrix} f_1'(z_1) \\ f_2'(z_2) \end{bmatrix} \right] \tag{5}$$

(Re) denotes the real part of a complex variable and a prime $(')$ shows the derivative with respect to the associated arguments. The elements of complex matrices A, B and P for an aligned orthotropic material are defined as

$$\begin{aligned} &A_{1k} = S_{11}\mu_k^2 + S_{12} - S_{16}\mu_k \quad , \quad A_{2k} = S_{12}\mu_k + \frac{S_{22}}{\mu_k} - S_{26} \\ &B_{1k} = -\mu_k \quad , \quad B_{2k} = 1 \\ &P_{kk} = \mu_k \quad , \quad P_{jk} = 0.\,(j \neq k) \end{aligned} \tag{6}$$

where $S_{16} = S_{26} = 0$[20,21,38,]. Beom et al[32] modified the Stroh formalism by introducing the complex functions $g_j(z)$ defined as,

$$g(z) = \begin{bmatrix} g_1(z) \\ g_2(z) \end{bmatrix} = B \begin{bmatrix} f_1(z) \\ f_2(z) \end{bmatrix} \tag{7}$$

Here the complex function G(z) is designated as

$$G(z) = g'(z) = B \begin{bmatrix} f_1'(z) \\ f_2'(z) \end{bmatrix} \tag{8}$$

For an orthotropic material,

$$\Delta = iAB^{-1} = \begin{bmatrix} S_{11}(p_1+p_2) & i\left(\sqrt{S_{11}S_{22}}+S_{12}\right) \\ -i\left(\sqrt{S_{11}S_{22}}+S_{12}\right) & \dfrac{S_{22}(p_1+p_2)}{p_1p_2} \end{bmatrix} \tag{9}$$

where Δ is a Hermitian matrix and can be written in terms of two real matrices H and Q as

$$\Delta = H + iQ = \begin{bmatrix} S_{11}(p_1+p_2) & 0 \\ 0 & \dfrac{S_{22}(p_1+p_2)}{p_1p_2} \end{bmatrix} + i\begin{bmatrix} 0 & \left(\sqrt{S_{11}S_{22}}+S_{12}\right) \\ -\left(\sqrt{S_{11}S_{22}}+S_{12}\right) & 0 \end{bmatrix} \tag{10}$$

The matrix H is symmetric and positive definite and the matrix Q is antisymmetric.

Now consider a bimaterial solid consisting of two orthotropic materials. See Fig. 1a. Assume the principal axes of each material are coincident with the Cartesian coordinates axes, x_1 and x_2. For this bimaterial structure, two matrices (α, β) are required to define the stress fields at their interface[12,14] which are,

$$\alpha = \left(\overset{(1)}{H} + \overset{(2)}{H}\right)^{-1}\left(\overset{(2)}{H} - \overset{(1)}{H}\right) = \begin{bmatrix} \alpha_{11} & 0 \\ 0 & \alpha_{22} \end{bmatrix} \tag{11}$$

$$\beta = \left(\overset{(1)}{H} + \overset{(2)}{H}\right)^{-1}\left(\overset{(2)}{Q} - \overset{(1)}{Q}\right) = \begin{bmatrix} 0 & \beta_{12} \\ \beta_{21} & 0 \end{bmatrix} \tag{12}$$

where

$$\alpha_{11} = \frac{\overset{(2)}{H}_{11} - \overset{(1)}{H}_{11}}{\overset{(1)}{H}_{11} + \overset{(2)}{H}_{11}},\ \alpha_{22} = \frac{\overset{(2)}{H}_{22} - \overset{(1)}{H}_{22}}{\overset{(1)}{H}_{22} + \overset{(2)}{H}_{22}},\ \beta_{12} = \frac{\overset{(2)}{Q}_{12} - \overset{(1)}{Q}_{12}}{\overset{(2)}{H}_{11} + \overset{(1)}{H}_{11}},\ \beta_{21} = \frac{\overset{(2)}{Q}_{21} - \overset{(1)}{Q}_{21}}{\overset{(2)}{H}_{22} + \overset{(1)}{H}_{22}}$$

the superscript indicates the material number. The elements of matrices $\overset{(n)}{H}$ and $\overset{(n)}{Q}$ (n=1,2) are given by equation 10 and

$$\beta_{12}\beta_{21} = -\beta_0^2 \tag{13}$$

β_0 is a dimensionless bimaterial parameter. For an isotropic bimaterial case, α and β reduce to $\alpha = \begin{bmatrix} \alpha_0 & 0 \\ 0 & \alpha_0 \end{bmatrix}$, $\beta = \begin{bmatrix} 0 & \beta_0 \\ -\beta_0 & 0 \end{bmatrix}$ where α_0 and β_0 are Dundor parameters[41].

REVIEW OF THE RELATIONS BETWEEN J_k-INTEGRAL AND SIFS FOR DIFFERENT ENGINEERING MATERIALS

For a 2D in-plane linear or non-linear elastic material of unit thickness, the J_k-integrals are the line integrals evaluated along a counterclockwise contour (s) enclosing and shrinking onto the crack tip defined as

$$J_k \equiv \lim_{r\to 0} \oint_S \left(W n_k - t_j u_{j,k}\right) ds \qquad (14)$$

where j,k=1,2 . W is the SED, n_k are the components of the unit outward normal to the contour path, t_j and u_j are the traction and displacement components along the path. For a straight crack, J_1-integral is the SERR along the crack.

For a linear elastic, isotropic and homogeneous material in mixed mode fracture, the SIFs and J_k-integrals are related by the following relations[26],

$$J_1 = \frac{K_1^2 + K_2^2}{E}, \qquad J_2 = -\frac{2K_1K_2}{E} \qquad (15)$$

Malyshev and Salganik[27] were the first scientists to find an analytical expression relating J_1 and SIFs for interfacial cracks between two dissimilar homogeneous and isotropic materials as

$$J_1 = \frac{1}{2(\cosh \pi\varepsilon)^2}\left[\frac{1}{\overset{(1)}{E}} + \frac{1}{\overset{(2)}{E}}\right]\left(K_1^2 + K_2^2\right) \quad \text{where} \quad \frac{1}{\overset{(n)}{E}} = \begin{cases} \dfrac{1}{\overset{(n)}{E}} & \text{Plane stress} \quad (16) \\[2ex] \dfrac{1-\left(\overset{(n)}{\nu}{}^2\right)}{\overset{(n)}{E}} & \text{Plane strain} \quad (17) \end{cases}$$

where $\overset{(n)}{E}$ (n=1,2) is the modulus of elasticity of each material.

Using the complex variable method, Gosz et al[28] and Khandelwal and Chadra Kishen[29] showed that J_2-integral can also be expressed in terms of the SIFs for interfacial cracks between two dissimilar homogeneous and isotropic materials as

$$J_2 = -\frac{1}{4\pi\varepsilon(\cosh\pi\varepsilon)^2}\left[\frac{1}{\overset{(1)}{E}}\left(1-e^{-2\pi\varepsilon}\right)+\frac{1}{\overset{(2)}{E}}\left(e^{2\pi\varepsilon}-1\right)\right]\times \left[\left(K_1^2-K_2^2\right)\sin(2\varepsilon\ln r)+2K_1K_2\cos(2\varepsilon\ln r)\right] \tag{18}$$

Equation 18 shows that J_2 depends on r, has an oscillatory variation and is non-existent when $r \to 0$.

Wang et al[30] and Chu and Hong[31] showed that the J_k-integral of a crack in an in-plane homogeneous and anisotropic structure can be related to the corresponding SIFs by

$$J_1 = a_{11}K_1^2 + a_{12}K_1K_2 + a_{22}K_2^2 \tag{19}$$

$$J_2 = b_{11}K_1^2 + b_{12}K_1K_2 + b_{22}K_2^2 \tag{20}$$

where the coefficients a_{jk} and b_{jk} are defined in appendix A.

Wuo[8] and Suo[11] presented an analytical expression for J_1 for an interfacial crack between two orthotropic bimaterial solids as

$$J_1 = \frac{1}{4(\cosh\pi\varepsilon)^2}\left[\left(\overset{(2)}{H}_{11}+\overset{(1)}{H}_{11}\right)K_2^2+\left(\overset{(2)}{H}_{22}+\overset{(1)}{H}_{22}\right)K_1^2\right] \tag{21}$$

Equations 14-21 have been used by academics and industrialists worldwide in relation to the fracture analyses of engineering structures. At present, there is no analytical expression relating J_2 and the SIFs for cracks between dissimilar anisotropic or orthotropic solids.

INTERFACIAL CRACK BETWEEN ORTHOTROPIC SOLIDS AND INTERFACE SIFS

Fig. 1b shows a straight crack lying along the interface between two linear elastic, homogeneous and orthotropic solids, of materials (1) and (2), respectively. The Cartesian coordinate system (x_1, x_2) has its origin (o) at the tip of the crack and the interface is assumed to be bonded perfectly. The crack and the interface both lie along the x_1-axis. The principal axes of both materials are assumed to be coincident with x_1 and x_2.

The complex analytical functions generating the singular fields near the tip of an interface crack between two dissimilar orthotropic materials can be expressed as[8,9,12,14,32]

$$\overset{(n)}{G}(z) = \frac{1}{2\sqrt{2\pi z}}\left(I + \Omega i\beta\right)\mathrm{Y}\left(z^{i\varepsilon}, z^{-i\varepsilon}\right)K \qquad (22)$$

Ω is equal to +1 and -1 for materials 1 and 2, respectively. I is a unit matrix and ε is an oscillatory bimaterial index defined as

$$\varepsilon = \frac{1}{2\pi}\mathrm{Ln}\frac{1+|\beta_0|}{1-|\beta_0|} \qquad (23)$$

K is the vector of interface SIFs and Y is the complex matrix function representing the oscillatory field. K and Y are defined as

$$\mathrm{Y}\left(z^{i\varepsilon}, z^{-i\varepsilon}\right) = \frac{1}{2}\left(z^{i\varepsilon-\frac{1}{2}} + z^{-i\varepsilon-\frac{1}{2}}\right)I + \frac{i}{2|\beta_0|}\left(z^{i\varepsilon-\frac{1}{2}} - z^{-i\varepsilon-\frac{1}{2}}\right)\beta \qquad (24)$$

$$K = \begin{bmatrix} K_2 \\ K_1 \end{bmatrix} = \lim_{x_1 \to 0}\sqrt{2\pi x_1}\,Y\left(x_1^{-i\varepsilon}, x_1^{i\varepsilon}\right)\begin{bmatrix} \sigma_{21}(x_1,0) \\ \sigma_{22}(x_1,0) \end{bmatrix} \qquad (25)$$

Substituting equations 12 and 24 into equation 22 and designating the complex functions D_1, D_2, $\overset{(n)}{\psi}$, $\overset{(n)}{\phi}$ as

$$D_1(z) = z^{i\varepsilon-\frac{1}{2}} + z^{-i\varepsilon-\frac{1}{2}}, \; D_2(z) = z^{i\varepsilon-\frac{1}{2}} - z^{-i\varepsilon-\frac{1}{2}},$$

$$\overset{(n)}{\psi}(z) = D_1(z) + \Omega|\beta_0|D_2(z), \quad \overset{(n)}{\phi}(z) = \Omega D_1(z) + \frac{D_2(z)}{|\beta_0|} \qquad (26)$$

Equation 22 becomes,

$$\overset{(n)}{G}(z) = \frac{1}{4\sqrt{2\pi}}\begin{bmatrix} \overset{(n)}{\psi}(z) & i\beta_{12}\overset{(n)}{\phi}(z) \\ i\beta_{21}\overset{(n)}{\phi}(z) & \overset{(n)}{\psi}(z) \end{bmatrix}\begin{bmatrix} K_2 \\ K_1 \end{bmatrix} \qquad (27)$$

Or

$$\overset{(n)}{G}(z) = \frac{1}{4\sqrt{2\pi}}\overset{(n)}{L}K \qquad (28)$$

where the complex matrix $\overset{(n)}{L}$ is defined as

$$\overset{(n)}{L} = \begin{bmatrix} \overset{(n)}{\psi}(z) & i\beta_{12}\overset{(n)}{\phi}(z) \\ i\beta_{21}\overset{(n)}{\phi}(z) & \overset{(n)}{\psi}(z) \end{bmatrix} \tag{29}$$

EVALUATION OF J_K-INTEGRALS FOR DEBONDED ORTHOTROPIC SOLIDS USING THE COMPLEX FUNCTUION METHOD

As mentioned earlier, an analytical expression for J_1 (Eq. 21) in debonded orthotropic bimaterials is already available. However, for the sake of clarity here, J_1 is also derived using the complex function method. Figs. 2a-b show two narrow rectangular contours s_1 and s_2 for evaluation of J_1 and J_2, respectively[42]. Based on these contours, equation 14 for J_1 and J_2 can be reduced to

$$J_1 = -\lim_{\substack{R\to 0.\\ \delta/R\to 0}} \oint_{s_1} \left(\sigma_{j2}^T u_{j,1}\right)(n_2)ds \tag{30}$$

$$J_2 = -\lim_{\substack{R\to 0.\\ \delta/R\to 0}} \oint_{s_2} \left(\sigma_{j1}^T u_{j,2}\right)(n_1)ds \tag{31}$$

As shown in Fig. 2a, for contour s_1, $x_2 \approx 0$, therefore

$$z_1 = z_2 = z \ , \ (n_2)ds = -dz \tag{32}$$

Based on equations 3, 4, 8, 9 and 22, the stress and displacement derivative vectors for each material are

$$\left(\sigma_{j2}^T\right)^{(n)} = 2\,\mathrm{Re}[G(z)]^{(n)} = \left(G(z) + \overline{G(z)}\right)^{(n)} \tag{33}$$

$$\left(u_{j,1}\right)^{(n)} = \begin{bmatrix} \dfrac{\partial u_1}{\partial x_1} \\ \dfrac{\partial u_2}{\partial x_1} \end{bmatrix}^{(n)} = 2\,\mathrm{Re}\left\{AB^{-1}G(z)\right\}^{(n)} = \left(-i\Delta G(z) + i\overline{\Delta}\overline{G(z)}\right)^{(n)} \tag{34}$$

Substituting equations 32-34 into equation 30 gives

$$J_1 = -\oint \left(G^T(z) + \overline{G^T(z)}\right)^{(n)} \left(-i\Delta G(z) + i\overline{\Delta}\overline{G(z)}\right)^{(n)} dz \tag{35}$$

As shown in Fig. 1b, for material-1, $0 \le \theta \le \pi$, and for material-2, $-\pi \le \theta \le 0$.

According to the complex integrals (B-1) shown in Appendix B, for $c_1 = c_2 = c = 1$, equation 35 can be written as

$$J_1 = i\oint\left(G^T(z)\Delta G(z) - \overline{G(z)}^T\,\overline{\Delta}\,\overline{G(z)}\right)^{(n)} dz \tag{36}$$

or

$$J_1 = -2\,\mathrm{Im}\left\{\oint\left[G^T(z)\Delta G(z)\right]^{(n)} dz\right\} \tag{37}$$

Substituting equation 28 into equation 37 we have,

$$J_1 = -\frac{1}{16\pi}\,\mathrm{Im}\left[\oint\left(K^T\,\overset{(n)}{L^T}\,\overset{(n)}{\Delta}\,\overset{(n)}{L}\,K\right)dz\right] \tag{38}$$

Inserting the elements of matrices L and Δ into equation 38, J_1 becomes

$$J_1 = -\frac{1}{16\pi}\oint\left\{K_2^2\left[\overset{(n)}{H}_{11}\overset{(n)}{\psi^2}(z) - \overset{(n)}{H}_{22}\beta_{21}^2\overset{(n)}{\phi^2}(z)\right] + K_1^2\left[\overset{(n)}{H}_{22}\overset{(n)}{\psi^2}(z) - \overset{(n)}{H}_{11}\beta_{12}^2\overset{(n)}{\phi^2}(z)\right]\right.$$

$$\left. + 2iK_1K_2\left[\beta_{12}\overset{(n)}{H}_{11} + \beta_{21}\overset{(n)}{H}_{22}\right]\overset{(n)}{\phi}(z)\overset{(n)}{\psi}(z)\right\}dz \tag{39}$$

Since $\beta_{12} = -\beta_{21}\dfrac{\overset{(1)}{H}_{22} + \overset{(2)}{H}_{22}}{\overset{(1)}{H}_{11} + \overset{(2)}{H}_{11}}$ and based on the complex integrals B-2 and C-1 shown in appendices B and C, respectively, equation 39 can be simplified to

$$J_1 = \frac{1}{4}\left(1-\beta_0^2\right)\left\{\left(\overset{(1)}{H}_{11} + \overset{(2)}{H}_{11}\right)K_2^2 + \left(\overset{(1)}{H}_{22} + \overset{(2)}{H}_{22}\right)K_1^2\right\} \tag{40}$$

Equation 40 is identical to equation 21.

The next stage is the derivation of J_2 using equation 31. As shown in Fig. 2b, for contour s_2, $x_1 \approx 0$, therefore,

$$z_1 = -i\mu_1 z\ ,\ z_2 = -i\mu_2 z\ \ ,(n_1 ds) = -idz \tag{41}$$

Based on equations 3 and 5, the stress and displacement derivative vectors for each material can be written as

$$\left(u_{j,2}\right)^{(n)} = \begin{bmatrix}\dfrac{\partial u_1}{\partial x_2}\\ \dfrac{\partial u_2}{\partial x_2}\end{bmatrix}^{(n)} = 2\,\mathrm{Re}\left\{AP\begin{bmatrix}f_1'(z_1)\\ f_2'(z_2)\end{bmatrix}\right\}^{(n)} \tag{42}$$

$$\left[\sigma_{j1}\right]^{(n)} = \begin{bmatrix}\sigma_{11}\\ \sigma_{21}\end{bmatrix}^{(n)} = -2\,\mathrm{Re}\left[BP\begin{bmatrix}f_1'(z_1)\\ f_2'(z_2)\end{bmatrix}\right]^{(n)} \tag{43}$$

By combining equations 8 and 27 we have,

$$\begin{bmatrix} f_1'(z) \\ f_2'(z) \end{bmatrix}^{(n)} = \left[B^{-1}G(z)\right]^{(n)} = \frac{1}{4\sqrt{2\pi}} \times \frac{1}{\overset{(n)}{\mu_2} - \overset{(n)}{\mu_1}} \begin{bmatrix} \left[\overset{(n)}{\psi}(z) + i\overset{(n)}{\mu_2}\beta_{21}\overset{(n)}{\phi}(z)\right]K_2 + \left[\overset{(n)}{\mu_2}\overset{(n)}{\psi}(z) + i\beta_{12}\overset{(n)}{\phi}(z)\right]K_1 \\ -\left[\overset{(n)}{\psi}(z) + i\overset{(n)}{\mu_1}\beta_{21}\overset{(n)}{\phi}(z)\right]K_2 - \left[\overset{(n)}{\mu_1}\overset{(n)}{\psi}(z) + i\beta_{12}\overset{(n)}{\phi}(z)\right]K_1 \end{bmatrix} \tag{44}$$

In order to evaluate the stress and displacement derivative vectors of each material using equations 42-43, $f_1'(z)$ and $f_2'(z)$ in the above relation must be written in terms of z_1 and z_2 , respectively, as

$$\begin{bmatrix} f_1'(z_1) \\ f_2'(z_2) \end{bmatrix}^{(n)} = \frac{1}{4\sqrt{2\pi}} \times \frac{1}{\overset{(n)}{\mu_2} - \overset{(n)}{\mu_1}} \begin{bmatrix} \left[\overset{(n)}{\psi}(z_1) + i\overset{(n)}{\mu_2}\beta_{21}\overset{(n)}{\phi}(z_1)\right]K_2 + \left[\overset{(n)}{\mu_2}\overset{(n)}{\psi}(z_1) + i\beta_{12}\overset{(n)}{\phi}(z_1)\right]K_1 \\ -\left[\overset{(n)}{\psi}(z_2) + i\overset{(n)}{\mu_1}\beta_{21}\overset{(n)}{\phi}(z_2)\right]K_2 - \left[\overset{(n)}{\mu_1}\overset{(n)}{\psi}(z_2) + i\beta_{12}\overset{(n)}{\phi}(z_2)\right]K_1 \end{bmatrix} \tag{45}$$

Next for the ease of integration, using equations 41 and the complex functions $\psi_j(z)$ and $\phi_j(z)$ (j=1,2) defined in appendix D, Eq. 45 can be written in the form,

$$\begin{bmatrix} f_1'(z_1) \\ f_2'(z_2) \end{bmatrix}^{(n)} = \frac{1}{4\sqrt{2\pi}} \times \frac{1}{\overset{(n)}{\mu_2} - \overset{(n)}{\mu_1}} \begin{bmatrix} \left(-i\overset{(n)}{\mu_1}\right)^{-\frac{1}{2}} \left\{\left[\overset{(n)}{\psi_1}(z) + i\overset{(n)}{\mu_2}\beta_{21}\overset{(n)}{\phi_1}(z)\right]K_2 + \left[\overset{(n)}{\mu_2}\overset{(n)}{\psi_1}(z) + i\beta_{12}\overset{(n)}{\phi_1}(z)\right]K_1\right\} \\ \left(-i\overset{(n)}{\mu_2}\right)^{-\frac{1}{2}} \left\{-\left[\overset{(n)}{\psi_2}(z) + i\overset{(n)}{\mu_1}\beta_{21}\overset{(n)}{\phi_2}(z)\right]K_2 - \left[\overset{(n)}{\mu_1}\overset{(n)}{\psi_2}(z) + i\beta_{12}\overset{(n)}{\phi_2}(z)\right]K_1\right\} \end{bmatrix} \tag{46}$$

By defining two new matrices $\overset{(n)}{q}$ and $\overset{(n)}{M}$ as

$$\overset{(n)}{q} = \begin{bmatrix} \frac{1}{\sqrt{\mu_1}(\mu_2 - \mu_1)} & 0 \\ 0 & \frac{1}{\sqrt{\mu_2}(\mu_2 - \mu_1)} \end{bmatrix}^{(n)} \tag{47}$$

$$\overset{(n)}{M} = \begin{bmatrix} \left[\overset{(n)}{\psi_1}(z) + i\overset{(n)}{\mu_2}\beta_{21}\overset{(n)}{\phi_1}(z)\right] & \left[\overset{(n)}{\mu_2}\overset{(n)}{\psi_1}(z) + i\beta_{12}\overset{(n)}{\phi_1}(z)\right] \\ -\left[\overset{(n)}{\psi_2}(z) + i\overset{(n)}{\mu_1}\beta_{21}\overset{(n)}{\phi_2}(z)\right] & -\left[\overset{(n)}{\mu_1}\overset{(n)}{\psi_2}(z) + i\beta_{12}\overset{(n)}{\phi_2}(z)\right] \end{bmatrix} \tag{48}$$

Equation 46 can be written in the form,

$$\begin{bmatrix} f_1'(z_1) \\ f_2'(z_2) \end{bmatrix}^{(n)} = \frac{1}{4\sqrt{2\pi}} \times \frac{1}{\sqrt{-i}} \times \overset{(n)}{q}\,\overset{(n)}{M}\,K \tag{49}$$

After substituting equation 49 into equations 42 and 43, the stress and displacement derivative vectors can be written as

$$[\sigma_{j1}]^{(n)} = \frac{-1}{4\sqrt{2\pi}} 2\,\mathrm{Re}\left[\frac{1}{\sqrt{-i}} \overset{(n)}{B}\,\overset{(n)}{P}\,\overset{(n)}{q}\,\overset{(n)}{M}\,K\right] = \frac{-1}{4\sqrt{2\pi}}\left(\frac{1}{\sqrt{-i}} \overset{(n)}{B}\,\overset{(n)}{P}\,\overset{(n)}{q}\,\overset{(n)}{M}\,K + \frac{1}{\sqrt{i}} \overset{(n)}{\overline{B}}\,\overset{(n)}{\overline{P}}\,\overset{(n)}{\overline{q}}\,\overset{(n)}{\overline{M}}\,K\right)$$

(50)

$$[u_{j,2}]^{(n)} = \frac{1}{4\sqrt{2\pi}} 2\,\mathrm{Re}\left[\frac{1}{\sqrt{-i}} \overset{(n)}{A}\,\overset{(n)}{P}\,\overset{(n)}{q}\,\overset{(n)}{M}\,K\right] = \frac{1}{4\sqrt{2\pi}}\left[\frac{1}{\sqrt{-i}} \overset{(n)}{A}\,\overset{(n)}{P}\,\overset{(n)}{q}\,\overset{(n)}{M}\,K + \frac{1}{\sqrt{i}} \overset{(n)}{\overline{A}}\,\overset{(n)}{\overline{P}}\,\overset{(n)}{\overline{q}}\,\overset{(n)}{\overline{M}}\,K\right]$$

(51)

In order to derive J_2, equations 50-51 are inserted into equation 31 and based on the complex integrals B-1 in Appendix B we have,

$$J_2 = \frac{1}{32\pi}\left[\oint\left(K^T \overset{(n)}{M^T}\,\overset{(n)}{q^T}\,\overset{(n)}{P^T}\,\overset{(n)}{B^T}\,\overset{(n)}{A}\,\overset{(n)}{P}\,\overset{(n)}{q}\,\overset{(n)}{M}\,K - K^T \overset{(n)}{\overline{M}^T}\,\overset{(n)}{\overline{q}^T}\,\overset{(n)}{\overline{P}^T}\,\overset{(n)}{\overline{B}^T}\,\overset{(n)}{\overline{A}}\,\overset{(n)}{\overline{P}}\,\overset{(n)}{\overline{q}}\,\overset{(n)}{\overline{M}}\,K\right)dz\right]$$

(52)

or

$$J_2 = 2\times\frac{-1}{32\pi}\,\mathrm{Im}\left[\frac{1}{i}\oint\left(K^T M^T q^T P^T B^T APqMK\right)dz\right] \qquad (53)$$

By designating the matrix ω_ε as

$$\omega_\varepsilon = q^T P^T B^T APq = \begin{bmatrix} \omega_{\varepsilon_{11}} & \omega_{\varepsilon_{12}} \\ \omega_{\varepsilon_{21}} & \omega_{\varepsilon_{22}} \end{bmatrix} \qquad (54)$$

Equation 53 can be written as

$$J_2 = -\frac{1}{16\pi}\,\mathrm{Im}\left[\frac{1}{i}\oint\left(K^T M^T \omega_\varepsilon MK\right)dz\right] \qquad (55)$$

As shown in appendix E, all the elements of the matrix ω_ε are real and depend mainly on the engineering constants and characteristic roots of the materials where

$$\omega_{\varepsilon_{11}} = .\frac{S_{22} - S_{11}\mu_1^4}{(\mu_2 - \mu_1)^2}$$

$$\omega_{\varepsilon_{22}} = \frac{S_{22} - S_{11}\mu_2^4}{(\mu_2 - \mu_1)^2} \qquad (56)$$

$$\omega_{\varepsilon_{12}} + \omega_{\varepsilon_{21}} = 0.$$

After substituting the elements of matrices q, M and ω_{ε} into equation 55, J_2 becomes

$$J_2 = -\frac{1}{16\pi}\,\mathrm{Im}\left\{\frac{1}{i}\oint\left[\left(\overset{(n)}{\omega}_{\varepsilon_{11}}\overset{(n)}{M}{}_{12}^{2}+\overset{(n)}{\omega}_{\varepsilon_{22}}\overset{(n)}{M}{}_{22}^{2}\right)K_1^2+\left(\overset{(n)}{\omega}_{\varepsilon_{11}}\overset{(n)}{M}{}_{11}^{2}+\overset{(n)}{\omega}_{\varepsilon_{22}}\overset{(n)}{M}{}_{21}^{2}\right)K_2^2 + 2\left(\overset{(n)}{\omega}_{\varepsilon_{11}}\overset{(n)}{M}_{11}\overset{(n)}{M}_{12}+\overset{(n)}{\omega}_{\varepsilon_{22}}\overset{(n)}{M}_{21}\overset{(n)}{M}_{22}\right)K_1K_2\right]dz\right\} \tag{57}$$

According to the complex integrals presented in appendix F, J_2 is derived as

$$J_2 = \Lambda_{\varepsilon_{11}}K_2^2 + \Lambda_{\varepsilon_{22}}K_1^2 + 2\Lambda_{\varepsilon_{12}}K_1K_2 \tag{58}$$

where

$$\begin{aligned}
\Lambda_{\varepsilon_{11}} &= \frac{1}{8\pi\varepsilon}\sum_{n=1}^{2}\left\{\overset{(n)}{\omega}_{\varepsilon_{11}}\left[\Omega\beta_0^2+\Omega\overset{(n)}{p}{}_2^2\beta_{21}^2-2\overset{(n)}{p}_2\beta_{21}\right]\sin 2\varepsilon\ln\overset{(n)}{p}_1 r+\overset{(n)}{\omega}_{\varepsilon_{22}}\left[\Omega\beta_0^2+\Omega\overset{(n)}{p}{}_1^2\beta_{21}^2-2\overset{(n)}{p}_1\beta_{21}\right]\sin 2\varepsilon\ln\overset{(n)}{p}_2 r\right\}\\
\Lambda_{\varepsilon_{22}} &= \frac{-1}{8\pi\varepsilon}\sum_{n=1}^{2}\left\{\overset{(n)}{\omega}_{\varepsilon_{11}}\left[\Omega\beta_{12}^2+\Omega\overset{(n)}{p}{}_2^2\beta_{0}^2+2\overset{(n)}{p}_2\beta_{12}\right]\sin 2\varepsilon\ln\overset{(n)}{p}_1 r+\overset{(n)}{\omega}_{\varepsilon_{22}}\left[\Omega\beta_{12}^2+\Omega\overset{(n)}{p}{}_1^2\beta_{0}^2+2\overset{(n)}{p}_1\beta_{12}\right]\sin 2\varepsilon\ln\overset{(n)}{p}_2 r\right\}\\
\Lambda_{\varepsilon_{12}} &= \frac{|\beta_0|}{8\pi\varepsilon}\sum_{n=1}^{2}\left\{\overset{(n)}{\omega}_{\varepsilon_{11}}\left[\Omega\beta_{12}-\Omega\overset{(n)}{p}{}_2^2\beta_{21}+2\overset{(n)}{p}_2\right]\cos 2\varepsilon\ln\overset{(n)}{p}_1 r+\overset{(n)}{\omega}_{\varepsilon_{22}}\left[\Omega\beta_{12}-\Omega\overset{(n)}{p}{}_1^2\beta_{21}+2\overset{(n)}{p}_1\right]\cos 2\varepsilon\ln\overset{(n)}{p}_2 r\right\}
\end{aligned} \tag{59}$$

Equation 58 is an analytical expression for J_2 in terms of SIFs for an in-plane traction free crack between two orthotropic elastic solids.

Equations 40 and 58 can be combined and then re-arranged with respect to K_1 and K_2 [25]. Once J_k values are obtained numerically using BEM or FEM, SIFs can be calculated. The signs of SIFs can be determined by checking the values of the crack opening displacements near the crack tip.

INTERFACIAL CRACK IN AN ORTHOTROPIC BIMATERIAL PLATE

An example of an interface crack between two dissimilar orthotropic materials is analysed to show the variation of J_2 in the vicinity of the crack tip. Different bimaterial combinations are considered to demonstrate the effect of elastic properties and material mismatch on J_k.

Fig. 3 shows a crack, with the length 2a=20mm, centred at the origin in a thin bimaterial plate consisting of Material-1 (top) and Material-2 (bottom) under a tensile stress of $\sigma_{y0} = 100MPa$. H and W are the width and height of the plate, respectively. It is assumed that a/W and H/W are small enough for the plate to be considered an infinite plate. The plane stress condition is also assumed. To ensure strain continuity along the bimaterial interface, in the infinite plate solution, $(\sigma_x)_0$ must be prescribed on the side of material-2, as shown in Fig. 3[2,25]. Table 1 shows the engineering constants for several composite materials[43]. As shown, seven different bimaterial combinations are arranged. Material-1 is designated as pitch graphite/epoxy (p-100/ERL-1962) and Material-2 varies from cases 1 to 7. The characteristic roots of each composite and the mismatch parameter ε for each bimaterial are also given in Table 1.

The exact analytical solution for SIFs of an infinite anisotropic bimaterial plate with a central interface crack is given by Qu and Bassani[10] as,

$$K = \sqrt{\pi a}\,\mathrm{Y}\left[(1+2i\varepsilon)(2a)^{-i\varepsilon}\right]\left[\sigma_{j2}\right]_0 \qquad (60)$$

where $(\sigma_{12})_0 = 0.$and $(\sigma_{22})_0 = \sigma_{y_0}$. For selected biamterial cases, the analytical values of J_2 are calculated using equations 58 and 60 when $10^{-6} \le \frac{r}{a} \le 10^{-3}$ and illustrated in Fig. 4. It can be observed that J_2 has a sharp variation near the crack tip and relatively a smooth change away from the crack tip.

Fig. 5 shows the variation of the J_k with respect to ε. J_2 curves are evaluated for $\frac{r}{a} = 10^{-6}, 10^{-5}, 10^{-4} \text{ and } 10^{-3}$. It can be observed that both J_1 and J_2 almost show the same trend of variation. Except for the bimaterial 3, the higher ε is the higher J_k is. Table 2 shows the SIF values of each bimaterial plate.

As discussed before, the J_k-integrals can be interpreted as the SERRs associated with the crack shape variation in the a_k directions. In a recent study by the author[24-25], the J_k values for isotropic bimaterials were successfully computed using BECSS and with the available analytical expressions the corresponding SIFs were calculated. Due to its generic application, that algorithm can be expanded to compute the J_k values of an interfacial crack in dissimilar orthotropic materials using BECSS. Using the analytical expression for the J_2-integral presented in this paper and in conjunction with the values of J_k, the corresponding SIFs for an in-plane traction free crack between two orthotropic elastic solids can be computed without the need for an auxiliary relation.

Although LEFM, based on the plane theory of elasticity, provides good approximate solutions for a wide range of engineering structures, in some cases 3D treatment of flaws can deliver more realistic and accurate results [44]. A comprehensive review of analytical, numerical and experimental research by Pook [45] shows the three-dimensional (3D) effects at cracks and sharp notches. This review [45] is mainly focused on linear elastic, homogeneous and isotropic materials. Therefore, further research is required to expand BECSS and its relevant analytical relations for the 3D analysis of LEIFM of anisotropic bimaterial structures.

The J_1-integral can also be employed for the analysis of notches in plane linear and nonlinear elasticity problems. Rice [16] showed that the J_1-integral at U-notches is also path-independent. The local strain energy density (SED) approach was originally proposed by Lazzarin and Zamabardi [46] for pointed and blunt V-notches subjected to uniaxial loading and subsequently was extended to muiltiaxial loadings [47]. They showed that the average value of SED in the small volume around a notch is a measure of the characterization of the initiation of fracture failure. Lazzarin et al [48] extended the J_1-integral concept from cracks to pointed V-notches. As both local SED and J_1 values characterize crack initiation at notches, Lazzarin et al [49] derived the relation between J_1 and local SED of sharp and blunt V-notches. Ref.[50] is a comprehensive review by Radaj on the local SED concept and its relation to the J_1-integral. Another option for further study is the application of BECSS and its relevant analytical relations for the analysis of notches in anisotropic homogeneous and bimaterial structures.

CONCLUSIONS

First, a brief review of LEIFM for in-plane anisotropic bimaterials has been made. Next, using the complex function method, an analytical expression between J_2-integral and the mixed-mode SIFs at the tip of an interface crack in debonded orthotropic elastic solids is presented. To the author's knowledge, this expression has not been previously published. Computation of J_1 is not adequate for calculation of SIFs. Using this analytical expression in conjunction with the values of J_1 and J_2 allows for the corresponding SIFs to be computed without the need for an auxiliary relation. Similar to the example presented in this paper, provided the SIFs are already available, by using this expression a very accurate value of J_2 can be obtained. This information can facilitate the prediction of the crack kink angle and propagation path of interface cracks in orthotropic bimaterials. Finally, an example with known analytical solutions for SIFs is presented to show the variation of J_2-integral near the crack tip of a bimaterial orthotropic plate using the available SIFs. Different bimaterial combinations are considered and the effect of material mismatch on J_k is demonstrated.

At present, the most commonly used method in industry for fracture analysis is the J_1-integral which is only applicable to straight cracks. Although it is less sensitive than the displacement method to the mesh size of the crack tip, it would still require stress analysis at internal points and fine contours around the crack front. Additionally, for mixed mode problems, auxiliary equations are required to separate SIFs. For an interfacial crack in anisotropic bimaterials, the displacement and traction data near the crack tip are usually employed to decouple and compute SIFs. In a recent study by the author, it was shown that the J_k-integrals can be interpreted as the SERRs associated with the crack shape variation in the a_k directions and can be computed using the BECSS for straight and curved cracks. Due to its generic application, that algorithm can be expanded to compute the J_k values of an interfacial crack in dissimilar anisotropic materials. With the analytical expression for the J_2-integral presented in this paper and in conjunction with the values of J_k computed using BECSS, the corresponding SIFs for an in-plane traction free crack between two orthotropic elastic solids can be obtained without the need for an auxiliary relation. In the future, it would be ideal to obtain an analytical expression for the J_2-integral of an interface crack in debonded anisotropic solids.

REFERENCES

1. Williams M.L. (1959) The stresses around a fault or crack in dissimilar media. Bull. Seismol. Soc. Am. 49c, 199-204.
2. Rice, J.R. and G.C. Sih (1965) Plane problems of cracks in dissimilar media. J. App. Mech. 32, 418-423.
3. Erdogan, F. (1963) Stress distribution in a nonhomogeneous elastic plane with cracks. Trans. ASME, J. Appl. Mech.,30, 232-236.
4. Erdogan, F. (1965) Stress distribution in bonded dissimilar materials with crack. J. Appl. Mech., 32, 403-409.
5. England, A.H. (1965) A crack between dissimilar media. ASME, J. Appl Mech., 32, 400-402.
6. Clements, D.L. (1971) A crack between dissimilar anisotropic media. Int. J. Engng Sci, 9, 257-265.
7. Willis, J.R. (1971) Fracture mechanics of interfacial crack. J. Mech. Phys. Solids, 19 , 353-368.
8. Wu, K.C. (1990) Stress intensity factor and energy release rate for interfacial cracks between dissimilar anisotropic materials. J. Appl. Mech., 57, 882-886.
9. Qu, J. and Li, Q. (1991) Interfacial dislocation and its application to interface cracks in anisotropic bimaterials. J. elasticity, 26, 169-195.
10. Qu, J., and Bassani J.L. (1993) Interfacial fracture mechanics for anisotropic bimaterials. J. Appl. Mech., 60, 422-431.
11. Suo, Z. (1990) Singularities, interfaces and cracks in dissimilar anisotropic media. Proc. R. Soc. Lond., A , 427, 331-358.
12. Ting, T.C.T. (1995) Generalized Dundors constants for anisotropic bimaterials. Int. J. Solids Struct., 32, 483-500.
13. Ting, T.C.T (1986) Explicit solution and invariance of the singularities at an interface crack in anisotropic composites. Int.J. Solids and Struct., 22, 965-983.

14. Beom, H. G. and Atluri, S.N. (1995) Dependence of stress on elastic constants in an anisotropic bimaterial under plane deformation; and the interfacial crack. Comput. Mech., 16, 106-113.
15. Banks-Sills, L. (2015) Interface fracture mechanics: theory and experiment. Int. J. of Fract., 191, 131-146.
16. Rice J.R. (1968) A path independent integral and the approximate analysis of strain concentration by notches and cracks. J Appl. Mech., 35, 379-386.
17. Rice, J.R. (1968) Mathematical Analysis in the Mechanics of Fracture. In: H. Liebowitz (Ed.), Treatise on Fracture, second ed., Academic Press, NY., , 191-311.
18. Tafreshi, A. (2009) Fracture Mechanics Analysis of Composite Structures Using the Boundary Element Shape Sensitivities. AIAA J, 47(8), 1926-1938.
19. Tafreshi, A. (2011) Simulation of crack propagation in anisotropic structures using the boundary element shape sensitivities and optimisation techniques. Engng. Anal. Bound. Elem. 35(8), 984-995.
20. Tafreshi, A. (2002) Shape design sensitivity analysis of 2D anisotropic structures using the boundary element method. Eng. Anal Bound Elem, 26(3), 237-251.
21. Tafreshi, A. (2005) Optimum shape design of composite structures using the boundary element method. AIAA J, 43(6), 1349-1359.
22. Tafreshi, A. (2009) Shape sensitivity analysis of composites in contact using the boundary element method. Engng. Anal Bound Elem, , 33(2), 215-224.
23. Tafreshi, A. (2006) Shape design sensitivity analysis with respect to the positioning of features in composite structures using the boundary element method. Engng. Anal. Bound. Elem, 30(1), 1-13.
24. Tafreshi A. (2015) Efficient evaluation of the J_2-integral using the boundary element crack shape sensitivities. Theoretical and applied fracture mechanics, 76, 9-16.
25. Tafreshi, A. (2016) Computation of the J_k-integrals for bimaterial interface cracks using boundary element crack shape sensitivities. Theoretical and applied fracture mechanics, 82,77-87.

26. Milne, I.; Ritchie, R.O., and Karihaloo, B. (Eds)(2003) Comprehensive structural integrity Vol.1-10. Elsevier 27.,B.M. Malyshev and R.L. Salganik (1965) . The strength of adhesive joints using the theory of fracture. Int. J. of Fract. Mech., 1, 114-128.

28. Gosz, M., Okyar, A.F. and Nair, S. (2003) A crack driving force criterion for the prediction of interface crack kinking in thin film composites. Interface Science, 11, 329-338.

29. Khandelwal, R. and Chadra Kishen, J.M. (2006) Complex variable method of computing Jk for bimaterial interface cracks. Engng. Fract. Mech, 73, 1568-1580.

30. Wang, S.S., Yau, J.F. and Corten, H.T. (1980) A mixed-mode crack analysis of anisotropic solids using conservation laws of elasticity. I.J. Fract. 16, 247-259.

31. Chu, S J and Hong, C S (1990) Application of the J_k integral to mixed mode crack problems for anisotropic composite laminates. Eng. Fract. Mech., 35(6), pp1093-1103.

32. Beom, H.G. and Cui, C.B. and Jang, H.S. (2012) Dependence of stress intensity factors on elastic constants for cracks in an orthotropic bimaterial with a thin film. Int. J. Solids Struct., 49, 3461-3471.

33. Chow, W.T., Beom, H.G. and Atluti, S.N. (1995) Calculation of stress intensity factors for an interfacial crack between dissimilar anisotropic media, using a hybrid element method and the mutual integral. Comput. Mech., 15, 546-557.

34. Song, C., Tin-Loi, F. and Gao, W. (2010) Transient dynamic analysis of interface cracks in anisotropic bimaterials by the scaled boundary finite-element method. Int. J. Solids Struct., 47, 978-989.

35. Ang, H.E., Torrance, J.E. and Tan, C.L. (1996) Boundary element analysis of orthotropic delamination specimens with interface cracks. Engng. Fract. Mech, 54(5), 601-615.

36. Ikeda, T., Nagai, M., Yamanaga, K. and Miyazaki, N. (2006) Stress intensity factor analyses of interface cracks between dissimilar anisotropic materials using the finite element method. Engng. Fract. Mech., 73, 2067-2079.

37. Jun, L., Garcia-Sanchez, F., Wunsche, M., Zhang,C., Wang,Y-S and Saez, A. (2009) Dynamic analysis of interfacial crack problems in anisotropic bimaterials by a time-domain BEM. Engng. Fract. Mech., 76, 1996-2010

38. Lekhnitskii, S.G. (1963) Theory of elasticity of an anisotropic elastic body. Holden-Day, San Fransisco.

39. Eshelby, J.D, Read, W.T., Shockley, W. (1953) Anisotropic elasticity with applications to dislocation theory. Acta Metall., 1, 251-259.

40. Stroh, A.N. (1958) Dislocation and cracks in anisotropic elasticity. Philos.. Mag. 3, 625-646.

41. Dundors, J. (1969) Discussion: edge-bonded dissimilar orthogonal elastic wedges under normal and shear loading. J. Applied Mech., 36: 650-656.

42. Cherepanov, G.P. (1979) Mechanics of brittle fracture. McGraw-Hill, New-York.

43. Gibson, R.F. (1994) Principles of composite material mechanics. McGraw-Hill, New York.

44. He, Z., Kotousov A. and Berto F. (2015) Effect of vertex singularities on stress intensities near plate free surfaces, Fatigue Fract. Engng Mater. Struct., 38: 860-869

45. Pook, L.P. (2013) A 50 year retrospective review of 3D effects at cracks and sharp notches, Fatigue Fract. Engng Mater. Struct., 36: 699-723

46. Lazzarin, P. and Zambardi, R. (2002) The equivalent strain energy density approach reformulated and applied to sharp V-shaped notches under localized and generalized plasticity. Fatigue Fract. Engng Mater. Struct., 25: 917-928

47. Lazzarin, P., Sonsino, C.M. and Zambardi, R. (2004) A notch stress intensity approach to assess the multiaxial fatigue strength of welded tube-to-flange joints subjected to combined loadings, Fatigue Fract. Engng Mater. Struct., 27, 127-140

48. Lazzarin, P., Livieri, P. and Zambardi, R. (2002) A J-integral based approach to predict the fatigue strength of components weakened by sharp V-shaped notches, Int. J. Comp. Appl. Techn., 15, 202-210

49. Berto, F. and Lazzarin, P. (2007) Relationships between J-integral and strain energy evaluated in a finite volume surrounding the tip of sharp and blunt V-notches, Int. J. Solids Struct., 44, 4621-4645

50. Radaj, D. (2015) State of the art review on the local strain energy density concept and its relation to the J-integral and peak stress method, Fatigue Fract. Engng Mater. Struct., 38, 2-28

Appendix A

$$a_{11} = -\frac{S_{22}}{2}\,\mathrm{Im}\left(\frac{\mu_1+\mu_2}{\mu_1\mu_2}\right) \qquad a_{22} = \frac{S_{11}}{2}\,\mathrm{Im}(\mu_1+\mu_2)$$

$$a_{12} = -\frac{S_{22}}{2}\,\mathrm{Im}\left(\frac{1}{\mu_1\mu_2}\right)+\frac{S_{11}}{2}\,\mathrm{Im}(\mu_1\mu_2) \qquad b_{11} = \frac{1}{2}\,\mathrm{Im}(\omega_{11}\omega_{21}+\omega_{31}\omega_{41})$$

$$b_{22} = \frac{1}{2}\,\mathrm{Im}(\omega_{12}\omega_{22}+\omega_{32}\omega_{42}) \qquad b_{12} = \frac{1}{2}\,\mathrm{Im}(\omega_{11}\omega_{22}+\omega_{12}\omega_{21}+\omega_{31}\omega_{42}+\omega_{32}\omega_{41})$$

A-1

The parameters ω_{lm} (l=1,4,m=1,2) are defined as

$$\omega_{11} = \frac{\mu_1\mu_2}{\mu_1-\mu_2}\left(-\frac{\mu_1}{\sqrt{\mu_1}}+\frac{\mu_2}{\sqrt{\mu_2}}\right),\ \omega_{12} = \frac{1}{\mu_1-\mu_2}\left(-\frac{\mu_1^2}{\sqrt{\mu_1}}+\frac{\mu_2^2}{\sqrt{\mu_2}}\right)$$

$$\omega_{21} = \frac{\mu_1\mu_2}{\mu_1-\mu_2}\left(-\frac{A_{11}}{\sqrt{\mu_1}}+\frac{A_{12}}{\sqrt{\mu_2}}\right),\ \omega_{22} = \frac{1}{\mu_1-\mu_2}\left(-\frac{A_{11}\mu_1}{\sqrt{\mu_1}}+\frac{A_{12}\mu_2}{\sqrt{\mu_2}}\right)$$

$$\omega_{31} = \frac{\mu_1\mu_2}{\mu_1-\mu_2}\left(-\frac{1}{\sqrt{\mu_1}}-\frac{1}{\sqrt{\mu_2}}\right),\ \omega_{32} = \frac{1}{\mu_1-\mu_2}\left(\frac{\mu_1}{\sqrt{\mu_1}}-\frac{\mu_2}{\sqrt{\mu_2}}\right)$$

$$\omega_{41} = \frac{\mu_1\mu_2}{\mu_1-\mu_2}\left(-\frac{A_{21}}{\sqrt{\mu_1}}+\frac{A_{22}}{\sqrt{\mu_2}}\right),\ \omega_{42} = \frac{1}{\mu_1-\mu_2}\left(-\frac{A_{21}\mu_1}{\sqrt{\mu_1}}+\frac{A_{22}\mu_2}{\sqrt{\mu_2}}\right)$$

A-2

Appendix B

$$z = re^{i\theta} \qquad dz = izd\theta$$

$$\int_0^\pi (c_1 z)^{-\frac{1}{2}+i\varepsilon} (c_2 \bar{z})^{-\frac{1}{2}+i\varepsilon} dz = \int_0^\pi (c_1 z)^{-\frac{1}{2}-i\varepsilon} (c_2 \bar{z})^{-\frac{1}{2}+i\varepsilon} dz = 0.$$

$$\int_0^\pi (c_1 z)^{-\frac{1}{2}+i\varepsilon} (c_2 \bar{z})^{-\frac{1}{2}-i\varepsilon} dz = \int_0^\pi (c_1 z)^{-\frac{1}{2}-i\varepsilon} (c_2 \bar{z})^{-\frac{1}{2}-i\varepsilon} dz = 0. \qquad \text{B-1}$$

$$\int_{-\pi}^0 (c_1 z)^{-\frac{1}{2}+i\varepsilon} (c_2 \bar{z})^{-\frac{1}{2}+i\varepsilon} dz = \int_{-\pi}^0 (c_1 z)^{-\frac{1}{2}-i\varepsilon} (c_2 \bar{z})^{-\frac{1}{2}+i\varepsilon} dz = 0.$$

$$\int_{-\pi}^0 (c_1 z)^{-\frac{1}{2}+i\varepsilon} (c_2 \bar{z})^{-\frac{1}{2}-i\varepsilon} dz = \int_{-\pi}^0 (c_1 z)^{-\frac{1}{2}-i\varepsilon} (c_2 \bar{z})^{-\frac{1}{2}-i\varepsilon} dz = 0.$$

$$\int_0^\pi z^{-1} dz = \int_{-\pi}^0 z^{-1} dz = i\pi$$

$$\int_0^\pi c^{2i\varepsilon} z^{2i\varepsilon-1} dz = \frac{i(cr)^{2i\varepsilon}|\beta_0|}{\varepsilon(1+|\beta_0|)} \qquad \int_{-\pi}^0 c^{2i\varepsilon} z^{2i\varepsilon-1} dz = \frac{i(cr)^{2i\varepsilon}|\beta_0|}{\varepsilon(1-|\beta_0|)} \qquad \text{B-2}$$

$$\int_0^\pi c^{-2i\varepsilon} z^{-2i\varepsilon-1} dz = \frac{i(cr)^{-2i\varepsilon}|\beta_0|}{\varepsilon(1-|\beta_0|)} \qquad \int_{-\pi}^0 c^{-2i\varepsilon} z^{-2i\varepsilon-1} dz = \frac{i(cr)^{-2i\varepsilon}|\beta_0|}{\varepsilon(1+|\beta_0|)}$$

where $(cr)^{2i\Omega\varepsilon} = \cos 2\varepsilon \,\mathrm{Ln}\, cr + \Omega i \sin 2\varepsilon \,\mathrm{Ln}\, cr$

Here c, c_1 and c_2 are constant real parameters. Ω is equal to +1 and -1 for materials 1 and 2, respectively.

Appendix C

Based on the definition of complex functions $\phi(z)$ and $\psi(z)$ given by equation (26), the following integrals are determined.

$$\int_{(n)} \overset{(n)}{\psi}{}^2 dz = \frac{2i|\beta_0|}{\varepsilon} \cos 2\varepsilon \,\mathrm{Ln}\, r - \frac{2\Omega\beta_0^2}{\varepsilon} \sin 2\varepsilon \,\mathrm{Ln}\, r + 2i\pi(1-\beta_0^2)$$

$$\int_{(n)} \overset{(n)}{\phi}{}^2 dz = \frac{2i}{\varepsilon|\beta_0|} \cos 2\varepsilon \,\mathrm{Ln}\, r - \frac{2\Omega}{\varepsilon} \sin 2\varepsilon \,\mathrm{Ln}\, r - \frac{2i\pi(1-\beta_0^2)}{\beta_0^2} \qquad \text{C-1}$$

$$\int_{(n)} \overset{(n)}{\phi} \overset{(n)}{\psi} dz = \frac{2i\Omega|\beta_0|}{\varepsilon} \cos 2\varepsilon \,\mathrm{Ln}(r) - \frac{2}{\varepsilon} \sin 2\varepsilon \,\mathrm{Ln}(r)$$

where n is the material number. It is assumed that for material 1, $0 \le \theta \le \pi$, and for material 2, $-\pi \le \theta \le 0$.

Appendix D

According to the definition of z_1 and z_2 given by equation 41, the complex functions $D_1(z_j), D_2(z_j), \psi(z_j), \phi(z_j), d_{1j}(z), d_{2j}(z), \psi_j(z), \phi_j(z)$ for each material are defined as

$$\overset{(n)}{D_1}(z_j) = \left(-i\overset{(n)}{\mu_j}\right)^{-\frac{1}{2}} \overset{(n)}{d_{1j}}(z)$$

$$\overset{(n)}{D_2}(z_j) = \left(-i\overset{(n)}{\mu_j}\right)^{-\frac{1}{2}} \overset{(n)}{d_{2j}}(z) \qquad \text{D-1}$$

$$\overset{(n)}{\psi}(z_j) = \left(-i\overset{(n)}{\mu_j}\right)^{-\frac{1}{2}} \overset{(n)}{\psi_j}(z)$$

$$\overset{(n)}{\phi}(z_j) = \left(-i\overset{(n)}{\mu_j}\right)^{-\frac{1}{2}} \overset{(n)}{\phi_j}(z)$$

where

$$\overset{(n)}{d_{1j}}(z) = \left[\overset{(n)}{p_j^{i\varepsilon}} z^{i\varepsilon-\frac{1}{2}} + \overset{(n)}{p_j^{-i\varepsilon}} z^{-i\varepsilon-\frac{1}{2}}\right]$$

$$\overset{(n)}{d_{2j}}(z) = \left[\overset{(n)}{p_j^{i\varepsilon}} z^{i\varepsilon-\frac{1}{2}} - \overset{(n)}{p_j^{-i\varepsilon}} z^{-i\varepsilon-\frac{1}{2}}\right] \qquad \text{D-2}$$

$$\overset{(n)}{\psi_j}(z) = \left[\overset{(n)}{d_{1j}}(z) + \Omega|\beta_0|\overset{(n)}{d_{2j}}(z)\right]$$

$$\overset{(n)}{\phi_j}(z) = \left[\Omega\overset{(n)}{d_{j1}}(z) + \frac{\overset{(n)}{d_{2j}}(z)}{|\beta_0|}\right]$$

Appendix E

$$\omega_\varepsilon = q^T.P^T.B^T.A.P.q = \begin{bmatrix} \omega_{\varepsilon_{11}} & \omega_{\varepsilon_{12}} \\ \omega_{\varepsilon_{21}} & \omega_{\varepsilon_{22}} \end{bmatrix} =$$

$$\begin{bmatrix} \dfrac{S_{22} - S_{11}\mu_1^4}{(\mu_2 - \mu_1)^2} & \dfrac{\mu_1 S_{22} + S_{12}\mu_1\mu_2(\mu_2 - \mu_1) - S_{11}\mu_1^2\mu_2^3}{\sqrt{\mu_1\mu_2}(\mu_2 - \mu_1)^2} \\ \dfrac{\mu_2 S_{22} - S_{12}\mu_1\mu_2(\mu_2 - \mu_1) - S_{11}\mu_1^3\mu_2^2}{\sqrt{\mu_1\mu_2}(\mu_2 - \mu_1)^2} & \dfrac{S_{22} - S_{11}\mu_2^4}{(\mu_2 - \mu_1)^2} \end{bmatrix}$$

E-1

where

$$\omega_{\varepsilon_{12}} + \omega_{\varepsilon_{21}} = \frac{(\mu_1 + \mu_2)(S_{22} - S_{11}\mu_1^2\mu_2^2)}{\sqrt{\mu_1\mu_2}(\mu_2 - \mu_1)^2}$$

Since $\mu_1\mu_2 = \sqrt{\dfrac{S_{11}}{S_{22}}}$, therefore, $\omega_{\varepsilon_{12}} + \omega_{\varepsilon_{21}}$ =0.

Appendix F

$$\int_{(n)} \overset{(n)}{M}{}_{11}^2\, dz = \int_{(n)} \left[\overset{(n)}{\psi}{}_1^2 + \left(\overset{(n)}{p}_2\right)^2 \beta_{21}^2 \overset{(n)}{\phi}{}_1^2 - 2\overset{(n)}{p}_2 \beta_{21} \overset{(n)}{\phi}_1 \overset{(n)}{\psi}_1 \right] dz$$

$$\int_{(n)} \overset{(n)}{M}{}_{21}^2\, dz = \int_{(n)} \left[\overset{(n)}{\psi}{}_2^2 + \left(\overset{(n)}{p}_1\right)^2 \beta_{21}^2 \overset{(n)}{\phi}{}_2^2 - 2\overset{(n)}{p}_1 \beta_{21} \overset{(n)}{\phi}_2 \overset{(n)}{\psi}_2 \right] dz \qquad \text{F-1}$$

$$\int_{(n)} \overset{(n)}{M}{}_{12}^2\, dz = -\int_{(n)} \left[\left(\overset{(n)}{p}_2\right)^2 \overset{(n)}{\psi}{}_1^2 + \beta_{12}^2 \overset{(n)}{\phi}{}_1^2 + 2\overset{(n)}{p}_2 \beta_{12} \overset{(n)}{\phi}_1 \overset{(n)}{\psi}_1 \right] dz$$

$$\int_{(n)} \overset{(n)}{M}{}_{22}^2\, dz = -\int_{(n)} \left[\left(\overset{(n)}{p}_1\right)^2 \overset{(n)}{\psi}{}_2^2 + \beta_{12}^2 \overset{(n)}{\phi}{}_2^2 + 2\overset{(n)}{p}_1 \beta_{12} \overset{(n)}{\phi}_2 \overset{(n)}{\psi}_2 \right] dz$$

$$\int_{(n)} \overset{(n)}{\psi}{}_j^2\, dz = \frac{2i\beta_0}{\varepsilon} \cos 2\varepsilon\, \mathrm{Ln}\left(\overset{(n)}{p}_j r\right) - \frac{2\Omega\beta_0^2}{\varepsilon} \sin 2\varepsilon\, \mathrm{Ln}\left(\overset{(n)}{p}_j r\right) + 2i\pi\left(1 - \beta_0^2\right)$$

$$\int_{(n)} \overset{(n)}{\phi}{}_j^2\, dz = \frac{2i}{\varepsilon\beta_0} \cos 2\varepsilon\, \mathrm{Ln}\left(\overset{(n)}{p}_j r\right) - \frac{2\Omega}{\varepsilon} \sin 2\varepsilon\, \mathrm{Ln}\left(\overset{(n)}{p}_j r\right) - \frac{2i\pi\left(1 - \beta_0^2\right)}{\beta_0^2} \qquad \text{F-2}$$

$$\int_{(n)} \overset{(n)}{\phi}_j \overset{(n)}{\psi}_j\, dz = \frac{2i\Omega\beta_0}{\varepsilon} \cos 2\varepsilon\, \mathrm{Ln}\left(\overset{(n)}{p}_j r\right) - \frac{2}{\varepsilon} \sin 2\varepsilon\, \mathrm{Ln}\left(\overset{(n)}{p}_j r\right)$$

Table 1 Typical values of lamina engineering constants for several composites[43]

	Case		E_1 (GPa)	E_2 (GPa)	G_{12} (GPa)	ν_{12}	μ_1	μ_2	ε
Material-1	N/A	p-100/ERL 1962 pitch Graphite/epoxy	468.9	6.2	5.58	0.31	9.082i	0.957i	N/A
Material-2	1	T300/934 Graphite/epoxy	131	10.3	6.9	0.22	4.222i	0.844i	0.0174
	2	AS/3501 Graphite/epoxy	138	9	6.9	0.3	4.309i	0.908i	0.0188
	3	Kevlar 49/934 aramid/epoxy	75.8	5.5	2.3	0.34	5.643i	0.657i	0.0374
	4	Scotchply 1002 E-glass/epoxy	38.6	8.27	4.14	0.26	2.870i	0.752i	0.0474
	5	Boron/5505 boron/epoxy	204	18.5	5.59	0.23	5.977i	0.555i	0.0069
	6	Spectra 900/826 Polyethylene/epoxy	30.7	3.52	1.45	0.32	4.483i	0.658i	0.0609
	7	E-glass/470-36 E-glass/vinylester	24.4	6.87	2.89	0.32	2.705i	0.696i	0.0553

Table 2 Stress intensity factors for each bimaterial plate with a central crack

Bimaterial No.	$K_1(MPa\sqrt{mm})$	$K_2(MPa\sqrt{mm})$
1	5.607E+02	-22.694
2	5.607E+02	-25.012
3	5.616E+02	-45.707
4	5.623E+02	-49.166
5	5.605E+02	-9.096
6	5.635E+02	-65.705
7	5.630E+02	-52.296

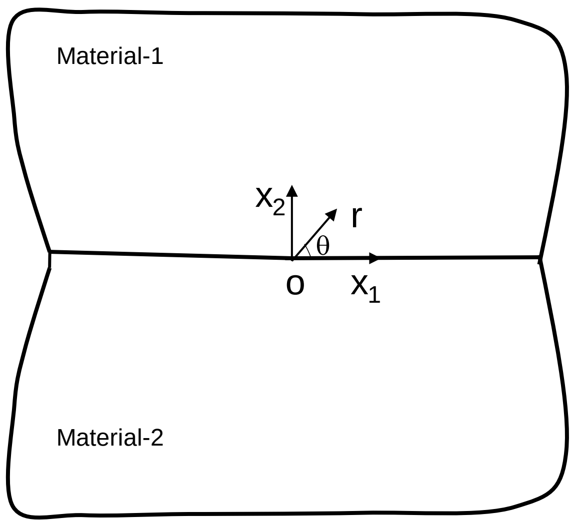

Figure 1a A bimaterial structure with an intact interface

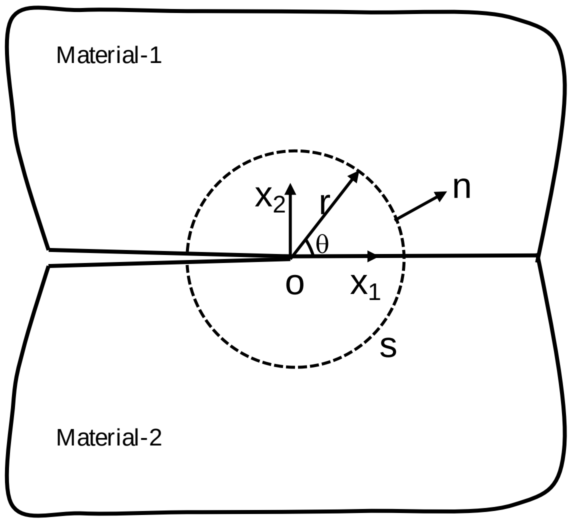

Figure 1b A bimaterial structure with an interface crack

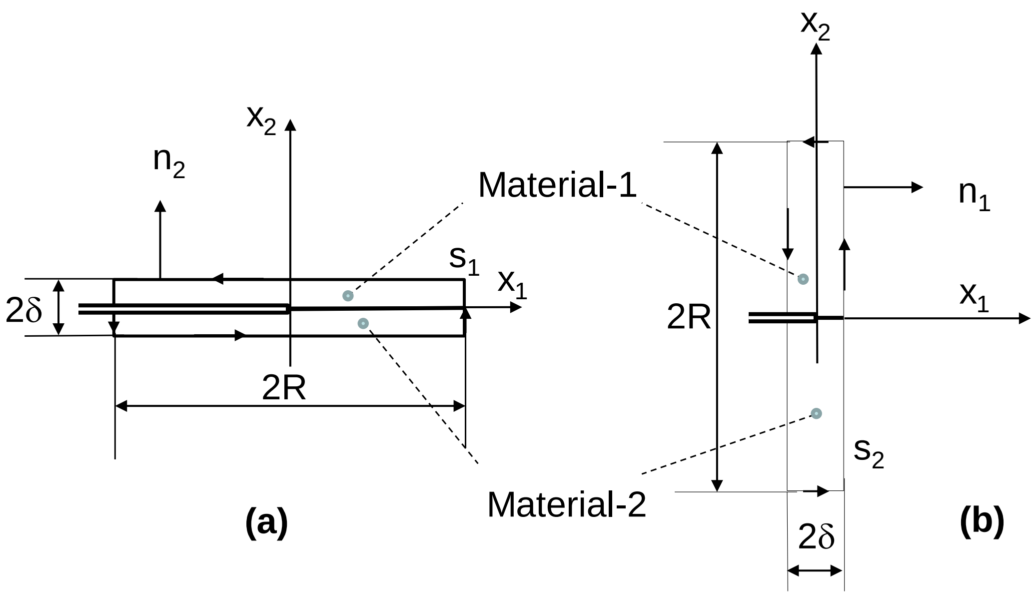

Figure 2 Narrow rectangular contours for calculation of the J_1 and J_2-integrals

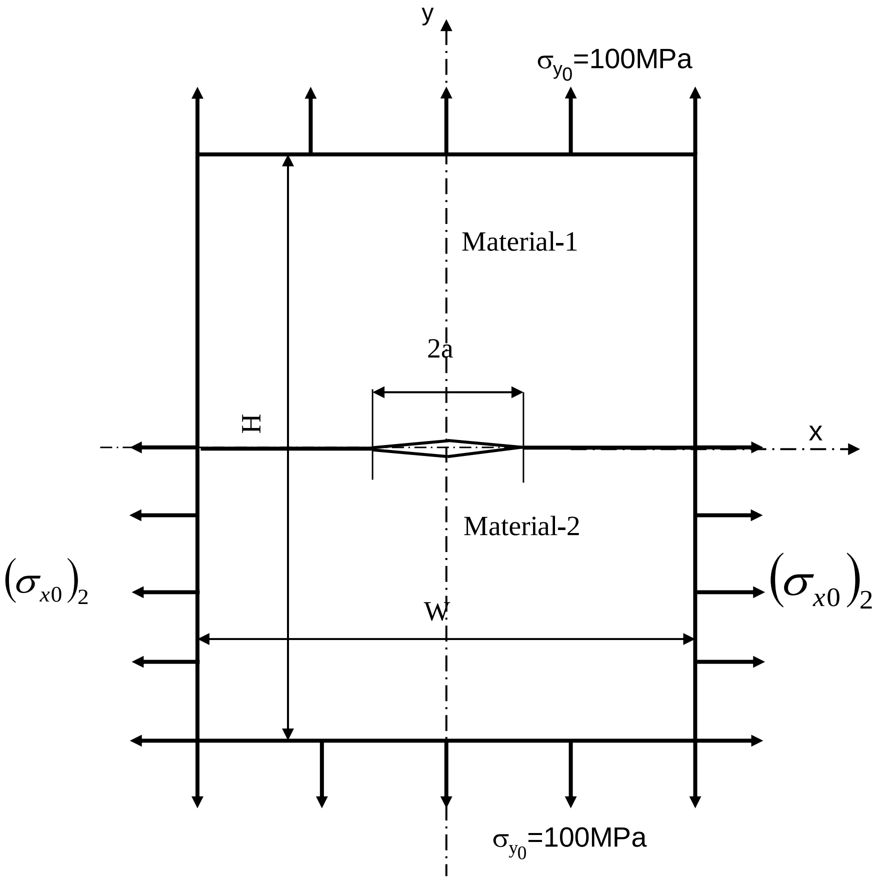

Figure 3 A bimaterial plate with an interface crack subject to tension

Fig. 4 Variation of the analytical values of $-J_2$-integral with respect to r/a for the plate with a central crack subject to tension for different bimaterial combinations

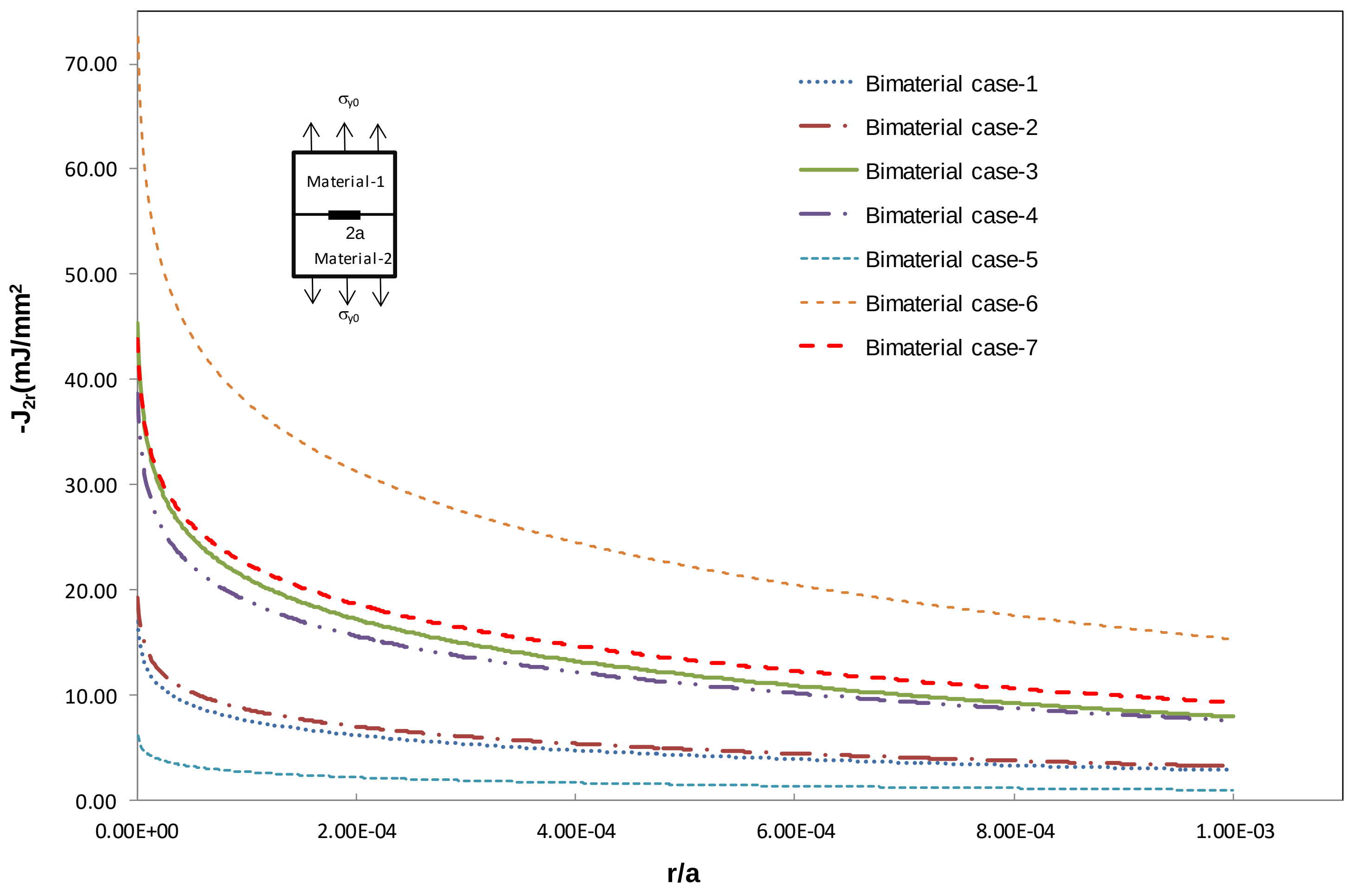

Fig. 5 Variation of the analytical values of J_1 and $-J_2$-integral for differenet values of r/a with respect to ε for the plate with a central crack subject to tension